CPV in $B^+ \to K^+\pi^-\pi^+$ decays

Nanyang Wang
on behalf of LHCb collaboration

CLHCP2026, 2026/10/30

Outline

- Introduction
- Amplitude analysis
- Physics results and implications
  - *CP* violation
  - Strong interaction modelling implications
- Conclusion

Introduction: *CP* violation

- **Direct CPV requires interfering amplitudes with different weak and strong phases**
  - Weak phases $\boldsymbol{\phi}$ from CKM matrix
  - Strong phases $\boldsymbol{\delta}$ from final-state interactions

$$A_{CP} = \frac{2|T||P|\sin(\delta_T - \delta_P)\sin(\phi_T - \phi_P)}{|T|^2 + |P|^2 + 2|T||P|\cos(\delta_T - \delta_P)\cos(\phi_T - \phi_P)}$$

$$A = |T|e^{i(\delta_T - \phi_T)} + |P|e^{i(\delta_P - \phi_P)}$$
$$\overline{A} = |T|e^{i(\delta_T + \phi_T)} + |P|e^{i(\delta_P + \phi_P)}$$

- Major milestones in CPV studies, **with no conclusive evidence of physics beyond the Standard Model**

- **Multi-body decays with amplitude analysis**
  - Rich resonant structure and interference
  - Access to additional observables: BFs, A_{CP} and relative phases for resonances

Introduction: Previous LHCb results

- Large localised CPV seen model-independently in $B^+ \to hh'h''(h = K, \pi)$ **PRD.108.012008(2023), Run2**

$B^+ \to \pi^+\pi^-\pi^+$ $B^+ \to \pi^+K^-K^+$ $B^+ \to K^+\pi^-\pi^+$ $B^+ \to K^+K^-K^+$

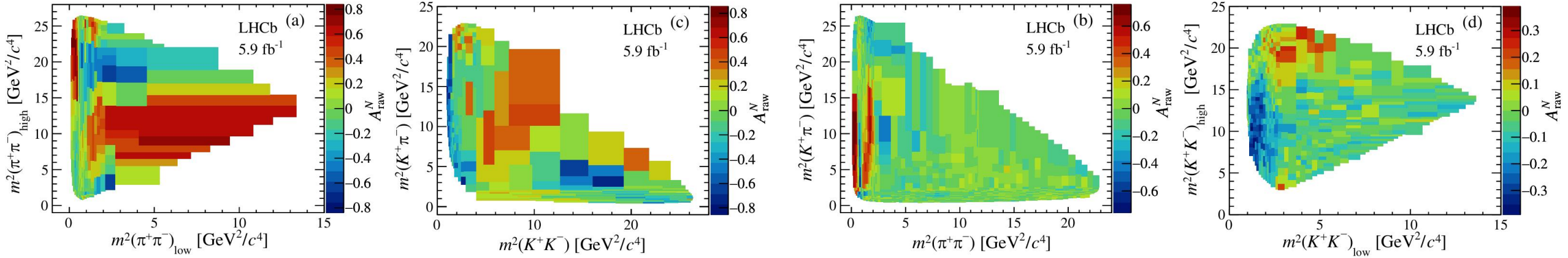

- Run 1 amplitude analysis: $B^+ \to \pi^+\pi^-\pi^+$ and $B^+ \to \pi^+K^-K^+$
  PRL.124.031801(2020) **PRL.123.231802(2019)**
  PRD.101.012006(2020)
- No previous LHCb amplitude analysis of $B^+ \to K^+\pi^-\pi^+$ and $B^+ \to K^+K^-K^+$
  - More challenging due to higher statistics
  - Need to model accurately subtle effects

Introduction: Previous results and puzzles

Puzzle 1: $\rho(770)^0$ CP asymmetry

- Evidence for CP violation in $B^+ \to \rho(770)^0 K^+$ seen in amplitude analysis by BaBar and Belle
- BaBar amplitude analysis: $A_{CP}^{\rho(770)^0} = (+0.44 \pm 0.11)$

PRD.78.012004(2008)

Apparent Discrepancy

- Model-independent determination of CPV in $\pi\pi$ P-Wave at the $\rho(770)$ peak, by LHCb PRD.108.012013(2023)
- $A_{CP}^{\rho\ window} = (+0.150 \pm 0.022)$

Puzzle 2: $K_0^*(1430)\pi$ Branching fraction

PRD.87.114001(2013)

- QCDf describes $B \to K_0^*(1430)^0[\eta', \rho, \omega, \phi]$, but predicts a much smaller $B^+ \to K_0^*(1430)^0\pi^+$ BF than measured in BaBar and Belle Eur.Phys.J.C.50.877(2007)

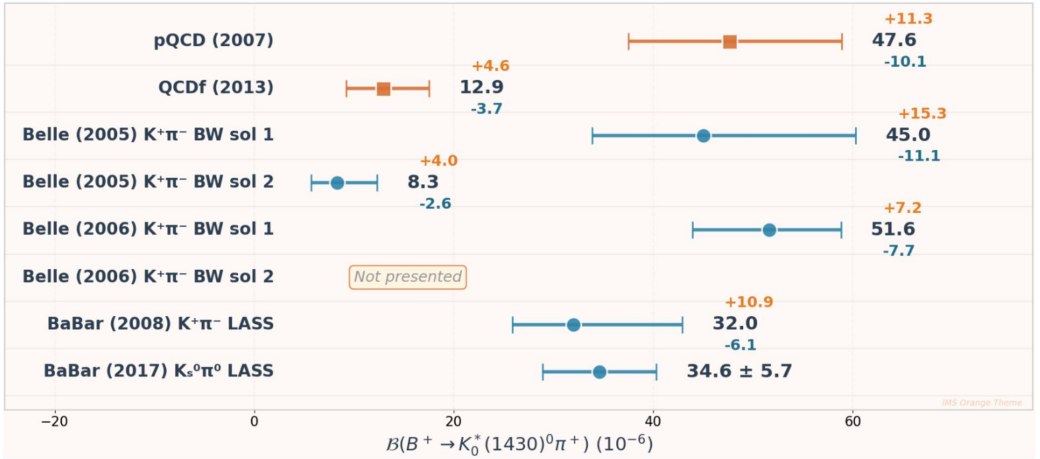

Puzzle 3: The mysterious $f_X(1300)$

- Belle and BaBar introduced a scalar $f_X(1300)$
- Freely parameterised $f_X(1300)$ gives **better fit quality** than $f_0(1370) + f_0(1500)$
- Fitted parameters consistent with $f_0(1370)$(Belle)/$f_0(1500)$(BaBar)

- If $f_X(1300) = f_0(1500)$
  - $B^+ \to f_0(1500)K^+$ BF from $B^+ \to K^+K^-K^+$ is $\sim 10 \times$ larger than implied by $B^+ \to K^+\pi^-\pi^+$
  - $f_0(1500)$ cannot dominate the $\pi^+\pi^-$ channel

PRD.85.112010(2012)

Outline

- Introduction
- Amplitude analysis
- Physics results and implications
  - *CP* violation
  - Strong interaction modelling implications
- Conclusion

Amplitude analysis: Isobar

- 3 alternative S-wave models, following strategy used in $B^+ \to \pi^+\pi^-\pi^+$
- 2 different fitters Laura++ and Mint2-devel in use, allows cross-checks
- **Isobar**
  - $K\pi$: effective-range-like (ER)+$K_0^*(1430)^0$, $K_0^*(1950)^0$
  - $\pi\pi$: $f_0(500)$, $f_0(980)$, $f_0(1370)$, $f_0(1500)$, $f_0(1710)$, rescattering

$$\mathcal{A}^{\pm}(\Phi_3) = \sum_j c_j^{\pm} F_j(\Phi_3)$$

Contribution	Approach	Mass lineshape	Fixed parameters
$(K^+\pi^-)_{\rm SVP}$	Isobar/K-matrix	GLASS (PRD78 034023)	—
$K_0^*(1430)^0$			
$K_0^*(1950)^0$	Isobar/K-matrix	Breit–Wigner	$m_0 = 1.945 \pm 0.022$ GeV/c^2 (PDG2020) $\Gamma_0 = 0.201 \pm 0.086$ GeV (PDG2020)
$f_0(500)$	Isobar	Bugg	fit (iii) (J. Phys. G34 151)
$f_0(980)$	Isobar	Flatté (PLB 63 224)	—
$f_0(1370)$	Isobar	T-matrix pole	$m_0 = 1.38 \pm 0.07$ GeV/c^2 (PRL130 051902) $\Gamma_0 = 0.22 \pm 0.08$ GeV (PRL130 051902)
$f_0(1500)$	Isobar	Breit–Wigner	$m_0 = 1.506 \pm 0.006$ GeV/c^2 (PDG2020) $\Gamma_0 = 0.112 \pm 0.009$ GeV (PDG2020)
$f_0(1710)$	Isobar	Breit–Wigner	$m_0 = 1.704 \pm 0.012$ GeV/c^2 (PDG2020) $\Gamma_0 = 0.123 \pm 0.018$ GeV (PDG2020)
$\pi\pi$-$\pi\pi$	Isobar	Rescattering	CFD (PRD83 074004)
$\pi\pi$-KK	Isobar	Rescattering	CFD_B (Phys. Rept. 969 1)
$\pi^+\pi^-$ S-wave	K-matrix	K-matrix	(PRD78 034023, EPJA16 229)
$K^+\pi^-$ and $\pi^+\pi^-$ S-waves	QMI	Constant per bin	—

Amplitude analysis: K-matrix

- K-matrix
  - $K\pi$: same as in Isobar approach
  - $\pi\pi$: 5 poles and slow-varying parts, 5 channels
    - Interface to scattering results, approach with unitary condition applied

Contribution	Approach	Mass lineshape	Fixed parameters
$(K^+\pi^-)_{\mathrm{SVP}}$	Isobar/K-matrix	GLASS (PRD78 034023)	—
$K_0^*(1430)^0$			
$K_0^*(1950)^0$	Isobar/K-matrix	Breit–Wigner	$m_0 = 1.945 \pm 0.022$ GeV/c^2 (PDG2020) $\Gamma_0 = 0.201 \pm 0.086$ GeV (PDG2020)
$f_0(500)$	Isobar	Bugg	fit (iii) (J. Phys. G34 151)
$f_0(980)$	Isobar	Flatté (PLB 63 224)	—
$f_0(1370)$	Isobar	T-matrix pole	$m_0 = 1.38 \pm 0.07$ GeV/c^2 (PRL130 051902) $\Gamma_0 = 0.22 \pm 0.08$ GeV (PRL130 051902)
$f_0(1500)$	Isobar	Breit–Wigner	$m_0 = 1.506 \pm 0.006$ GeV/c^2 (PDG2020) $\Gamma_0 = 0.112 \pm 0.009$ GeV (PDG2020)
$f_0(1710)$	Isobar	Breit–Wigner	$m_0 = 1.704 \pm 0.012$ GeV/c^2 (PDG2020) $\Gamma_0 = 0.123 \pm 0.018$ GeV (PDG2020)
$\pi\pi$-$\pi\pi$	Isobar	Rescattering	CFD (PRD83 074004)
$\pi\pi$-KK	Isobar	Rescattering	CFD_B (Phys. Rept. 969 1)
$\pi^+\pi^-$ S-wave	K-matrix	K-matrix	(PRD78 034023, EPJA16 229)
$K^+\pi^-$ and $\pi^+\pi^-$ S-waves	QMI	Constant per bin	—

Amplitude analysis: Quasi-Model-Independent

- Quasi-Model-Independent (QMI)
  - Simultaneous QMI treatment of the two crossing S-waves
  - $K\pi/\pi\pi$: 35/40 bins below charm, 15/10 above
  - Bin boundaries aligned with hadronic thresholds to capture expected cusps from rescattering effects

$K^+\pi^-$ $\pi^+\pi^-$

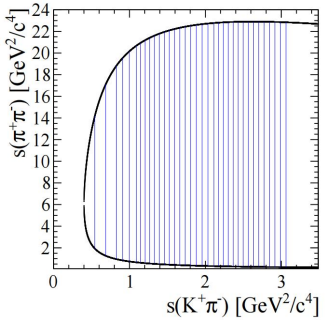

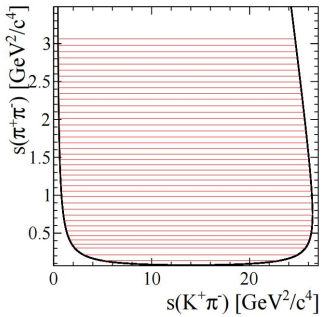

Contribution	Approach	Mass lineshape	Fixed parameters
$(K^+\pi^-)_{\mathrm{SVP}}$	Isobar/K-matrix	GLASS (PRD78 034023)	—
$K_0^*(1430)^0$			
$K_0^*(1950)^0$	Isobar/K-matrix	Breit–Wigner	$m_0 = 1.945 \pm 0.022$ GeV/c^2 (PDG2020) $\Gamma_0 = 0.201 \pm 0.086$ GeV (PDG2020)
$f_0(500)$	Isobar	Bugg	fit (iii) (J. Phys. G34 151)
$f_0(980)$	Isobar	Flatté (PLB 63 224)	—
$f_0(1370)$	Isobar	T-matrix pole	$m_0 = 1.38 \pm 0.07$ GeV/c^2 (PRL130 051902) $\Gamma_0 = 0.22 \pm 0.08$ GeV (PRL130 051902)
$f_0(1500)$	Isobar	Breit–Wigner	$m_0 = 1.506 \pm 0.006$ GeV/c^2 (PDG2020) $\Gamma_0 = 0.112 \pm 0.009$ GeV (PDG2020)
$f_0(1710)$	Isobar	Breit–Wigner	$m_0 = 1.704 \pm 0.012$ GeV/c^2 (PDG2020) $\Gamma_0 = 0.123 \pm 0.018$ GeV (PDG2020)
$\pi\pi$-$\pi\pi$	Isobar	Rescattering	CFD (PRD83 074004)
$\pi\pi$-KK	Isobar	Rescattering	CFD_B (Phys. Rept. 969 1)
$\pi^+\pi^-$ S-wave	K-matrix	K-matrix	(PRD78 034023, EPJA16 229)
$K^+\pi^-$ and $\pi^+\pi^-$ S-waves	QMI	Constant per bin	—

Outline

- Introduction
- Amplitude analysis
- Physics results and implications
  - *CP* violation
  - Strong interaction modelling implications
- Conclusion

Fit projection

LHCb-PAPER-2025-067

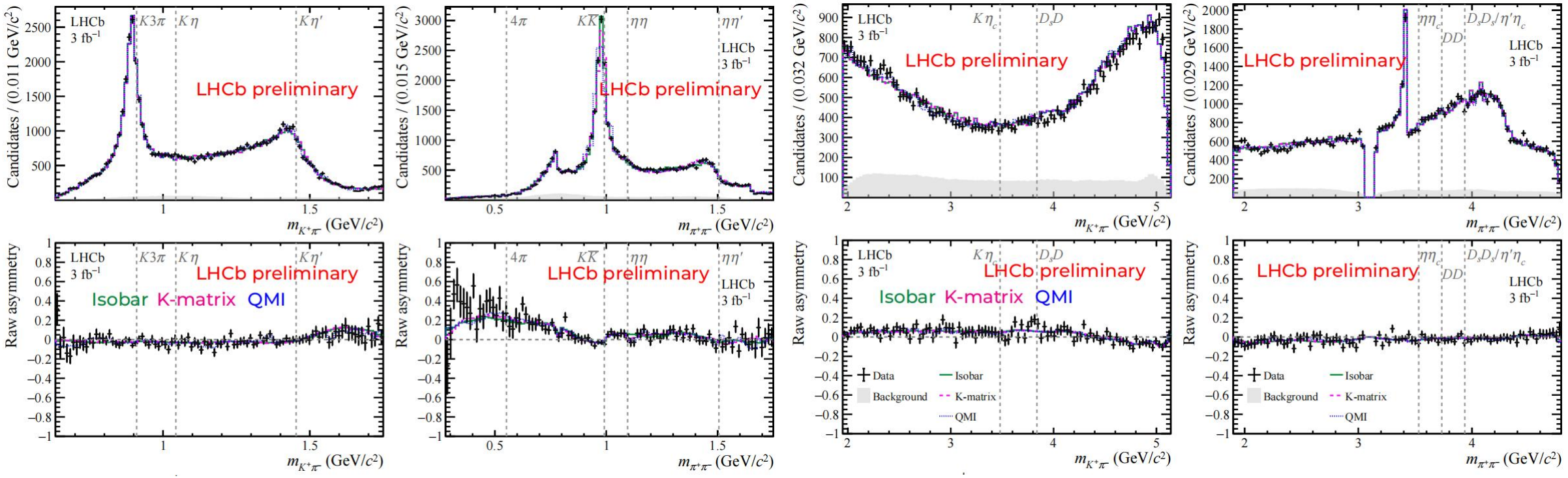

- Reasonable agreement between data and models: all three S-wave models with $\chi^2/\mathrm{ndf}\sim1.6$ without considering systematic uncertainties

CP violation results LHCb-PAPER-2025-069

- *CP* violation of individual component: $A_{CP}^{i} = \frac{F_i^- - F_i^+}{F_i^- + F_i^+}$
- *CP* violation of interference between two components: $A_I^{ij} = (I_{ij}^- - I_{ij}^+)/F_{ij}$

Parameter	Isobar	K-matrix	QMI
$\mathcal{A}_{CP}(K^*(892)^0)$	$-0.038 \pm 0.010 \pm 0.018$ (1.9σ)	$-0.035 \pm 0.012 \pm 0.017$ (1.7σ)	$-0.027 \pm 0.014 \pm 0.023$ (1.0σ)
$\mathcal{A}_{CP}(K_0^*(1430)^0)$	$-0.094 \pm 0.020 \pm 0.046$ (1.9σ)	$-0.121 \pm 0.015 \pm 0.050$ (2.3σ)	—
$\mathcal{A}_{CP}(\rho(770)^0)$	$+0.280 \pm 0.022 \pm 0.029$ (7.6σ)	$+0.271 \pm 0.022 \pm 0.015$ (10.2σ)	$+0.359 \pm 0.037 \pm 0.048$ (5.9σ)
$\mathcal{A}_{CP}^{S}(m_{\pi^+\pi^-} < 4m_\pi)$	$+0.665 \pm 0.032 \pm 0.053$ $(>10\sigma)$	$+0.638 \pm 0.008 \pm 0.016$ $(>10\sigma)$	$+0.754 \pm 0.115 \pm 0.113$ (4.7σ)
$\mathcal{A}_{\mathcal{I}}^{SD}$ $(\times 10^{-1})$	$+0.058 \pm 0.007 \pm 0.008$ (5.2σ)	$+0.055 \pm 0.007 \pm 0.007$ (5.3σ)	$+0.071 \pm 0.014 \pm 0.009$ (4.4σ)
$\mathcal{A}_{\mathcal{I}}^{SP}$ $(\times 10^{-1})$	$-0.237 \pm 0.018 \pm 0.040$ (5.4σ)	$-0.249 \pm 0.021 \pm 0.040$ (5.5σ)	$-0.253 \pm 0.025 \pm 0.028$ (6.7σ)
$\mathcal{A}_{CP}(\rho_3(1690)^0)$	$+0.603 \pm 0.090 \pm 0.121$ (4.0σ)	$+0.477 \pm 0.100 \pm 0.096$ (3.4σ)	$+0.698 \pm 0.135 \pm 0.163$ (3.3σ)

LHCb preliminary

- Angular distribution: a sum of Legendre polynomials

$$\frac{dN}{d\cos\theta} \propto 1 + \sum_{n=1}^{N} a_n P_n(\cos\theta)$$

helicity angle — Legendre moments

- Sensitivity of Legendre moments to partial-wave interference

$$\langle P_1 \rangle \propto SP\cos(\theta_S - \theta_P) + 2\sqrt{\tfrac{2}{5}}PD\cos(\theta_P - \theta_D)$$

$$\langle P_2 \rangle \propto \sqrt{\tfrac{2}{5}}P^2 + \sqrt{\tfrac{10}{7}}D^2 + \sqrt{2}SD\cos(\theta_S - \theta_D)$$

$$\Delta\langle P_n \rangle \equiv \langle P_n \rangle_{B^+} - \langle P_n \rangle_{B^-}$$

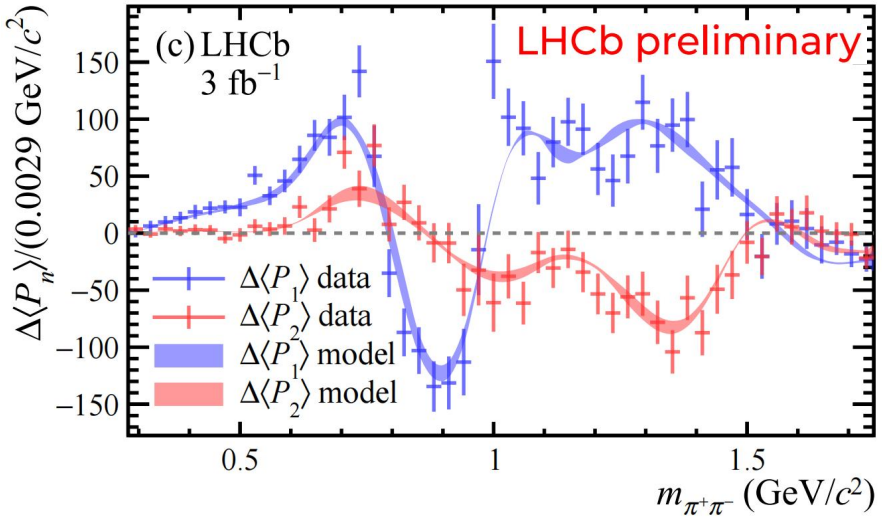

CP violation results: CPV in $\rho(770)^0 K^+$

Probably associated with known phase variation

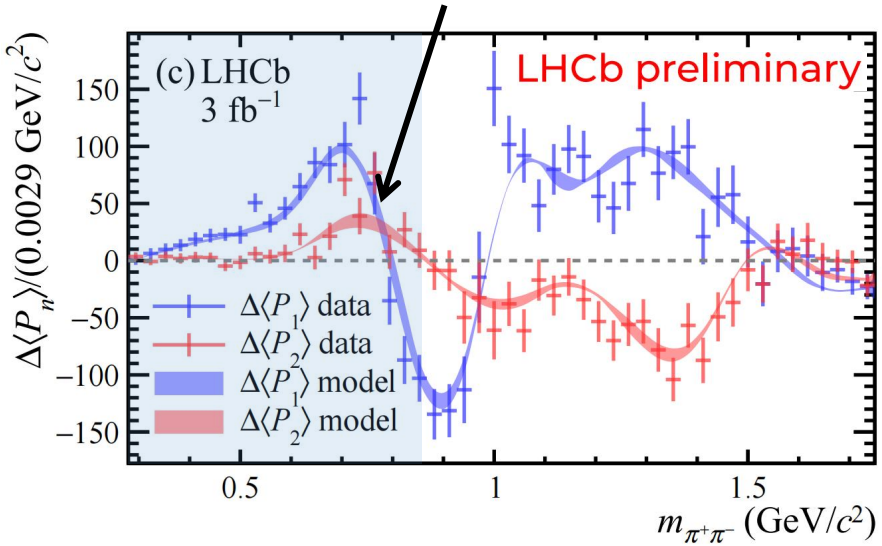

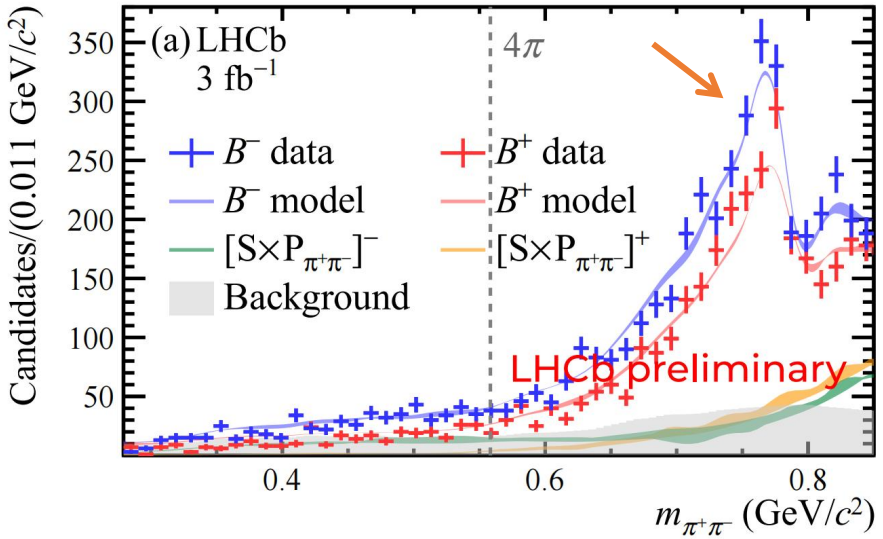

- Clear positive *CP* asymmetry for S-wave in $m_{\pi^+\pi^-} < 4m_\pi$
- Clear positive *CP* asymmetry for $\rho(770)^0$
- Observed *CP* violation in S-P interference, sign change around the $\rho(770)^0$ pole, very similar to $B^+ \to \pi^+\pi^-\pi^+$
- No significant CPV in ω and $\rho - \omega$ mixing contribution, diluting the overall asymmetry in the $\pi\pi$ P-wave

Explains puzzle 1: $\rho(770)^0$ CP asymmetry

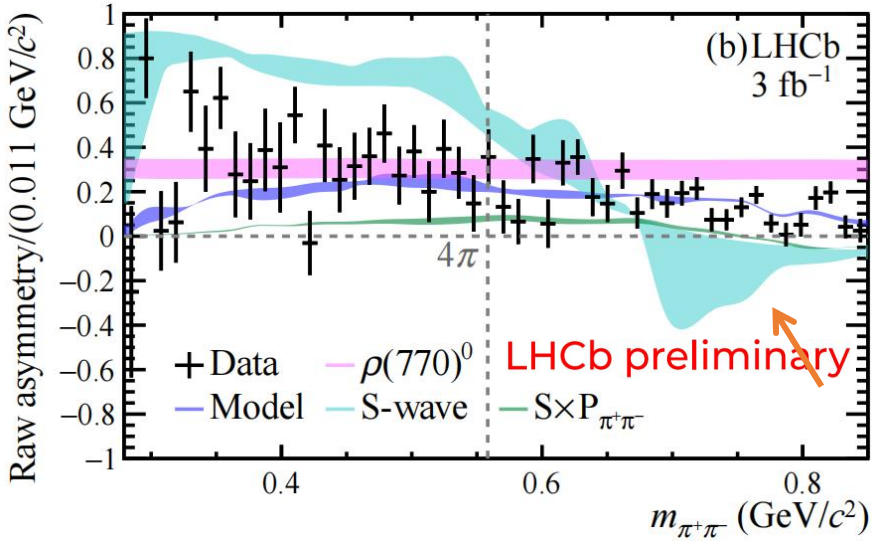

CP violation results: $f_2(1270)$ CPV

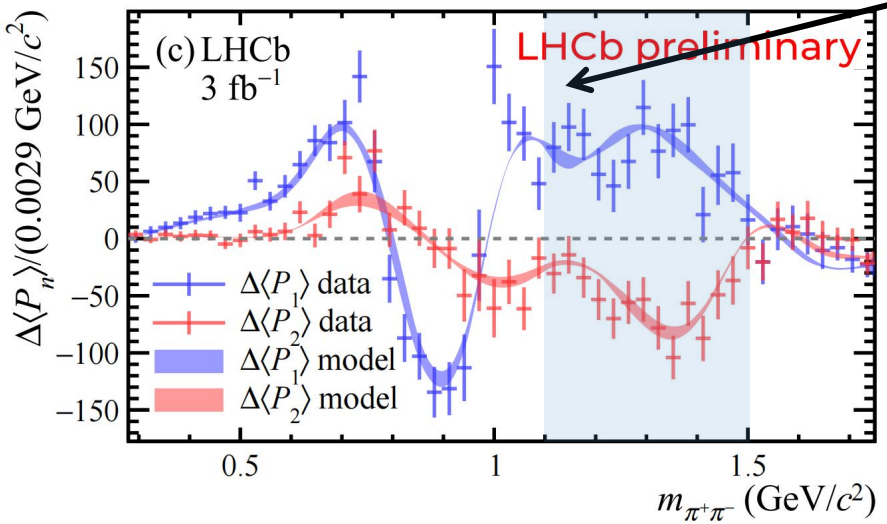

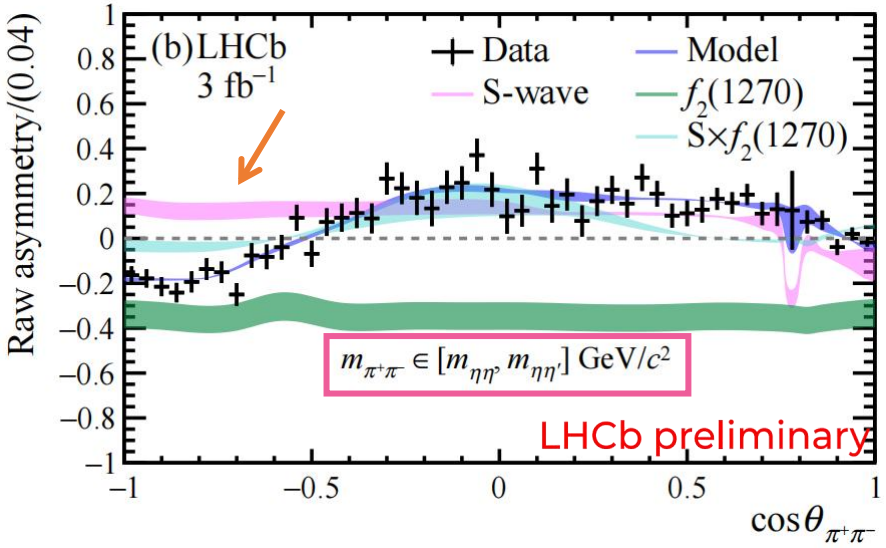

- Raw asymmetry in the $\pi\pi$ helicity angle in $f_2(1270)$ mass range
- $\cos\theta_{\pi^+\pi^-} < -0.5$: Negative *CP* asymmetry for $f_2(1270)$
- In other regions S-wave *CP* asymmetry cancels or dominates D-wave contribution
- S-D interference contributes to raw asymmetry
- 2D test shows CP conservation is rejected at minimum 8.2σ for three approaches
  - $\Delta x/\Delta y$: *CP*-violating Cartesian coefficients

$$c_j^{\pm} = (x_j \pm \Delta x_j) + i(y_j \pm \Delta y_j)$$

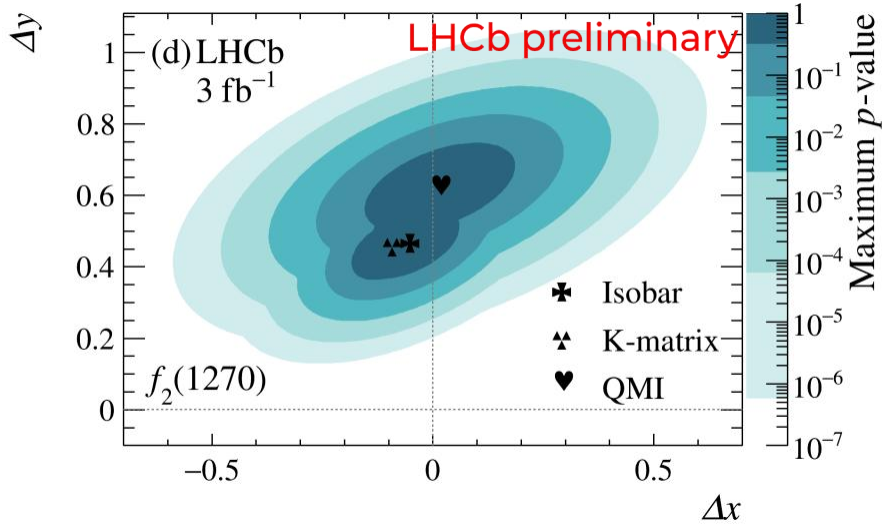

CP violation results: CPV in $\rho_3(1690)^0 K^+$

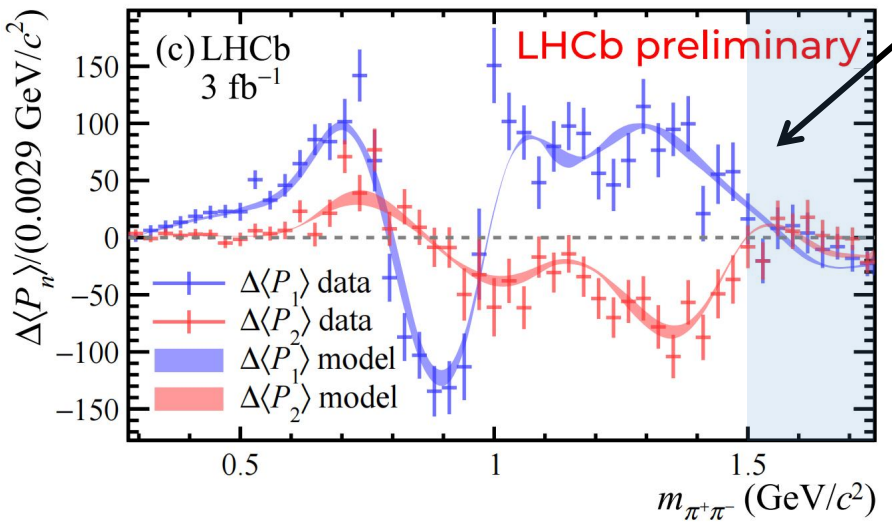

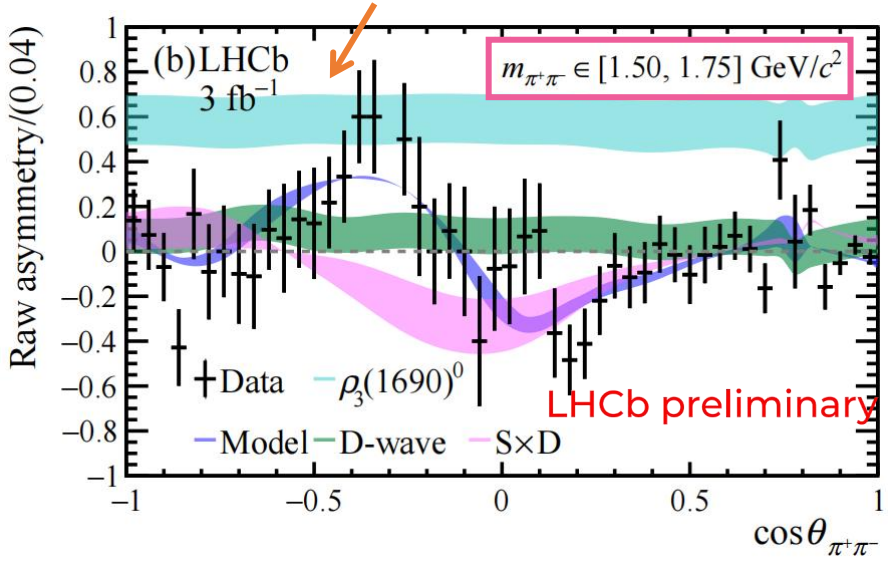

- Sizeable $\boldsymbol{\rho_3(1690)^0}$ contribute above 1.5 GeV
- $\cos\theta_{\pi^+\pi^-} \sim -0.5$: $\boldsymbol{\rho_3(1690)^0}$ responsible for the asymmetry
- S-D interference contribution near $\cos\theta_{\pi^+\pi^-} \sim 0$

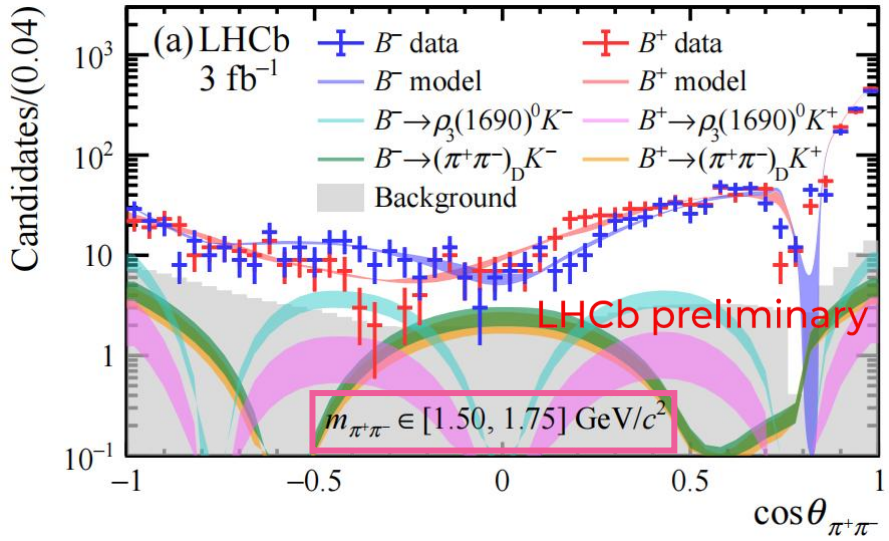

The $K_0^*(1430)\pi$ BF and $f_X(1300)$ Puzzles

- **Previous:**
  - Larger $B^+ \to K_0^*(1430)^0\pi^+$ BF favour pQCD
  - QCDf describes $B \to K_0^*(1430)[\eta', \rho, \omega, \phi]$
  - $f_X\,(1300)$
- **Belle and BaBar:** used BW or LASS shapes, relying on unitary-based arguments in the charmless $K\pi$ S-wave
- **LHCb:** GLASS allows independent coupling between the resonant and effective-range components, relaxing the LASS constraints.
- **Resolution:**
  - The smaller $K_0^*(1430)$ contribution obtained with GLASS leads to a BF consistent with QCDf, removing the previous preference for pQCD
  - **No $f_X(1300)$ required:** Improved $K\pi$ S-wave model describes data with the established $f_0(1370)$ and $f_0(1500)$

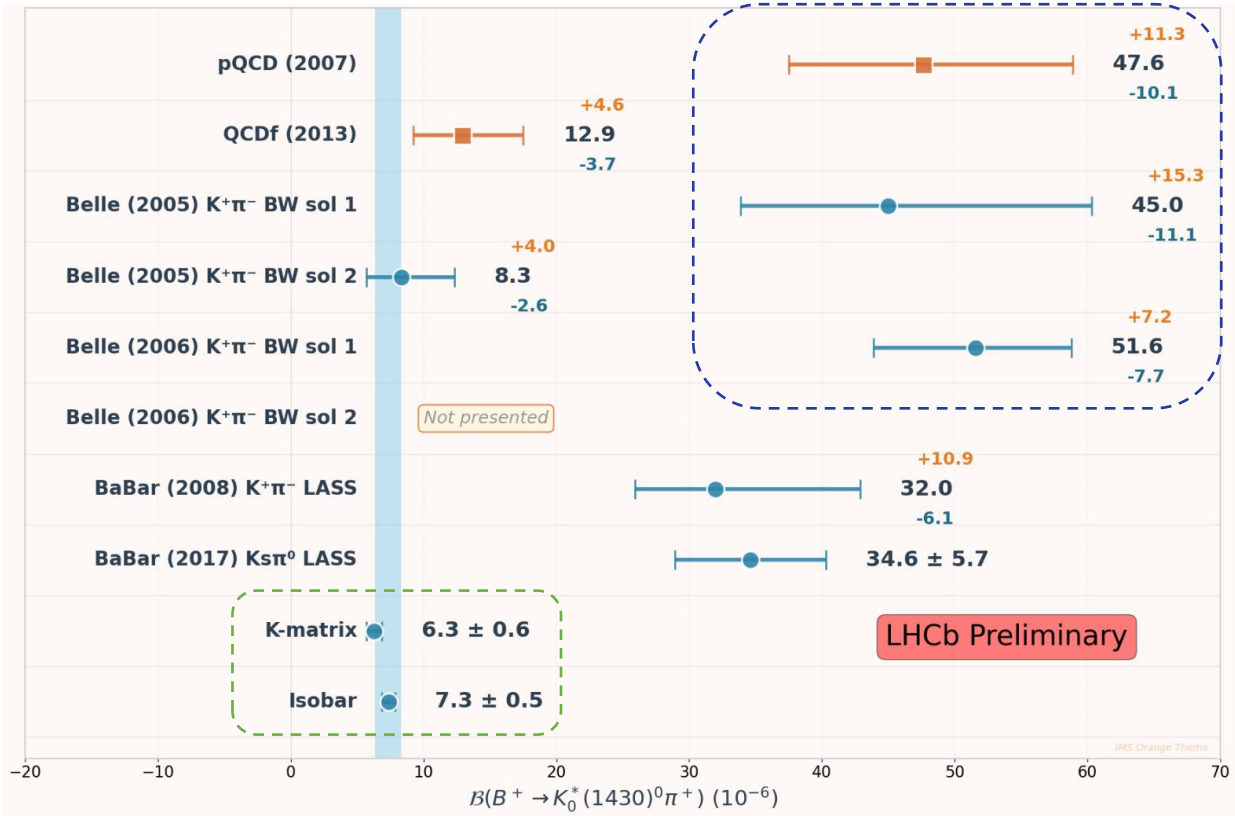

Explains puzzle 2

Explains puzzle 3

New intermediate processes

- **Measure significance of each resonance**
- Two approaches:
  - Fit fraction z-score
  - 2D deviation of amplitude coupling from (0,0)
- Ten intermediate processes are observed for the first time
- $\pi\pi$-$\pi\pi$ rescattering help Isobar achieve better fit quality than K-matrix

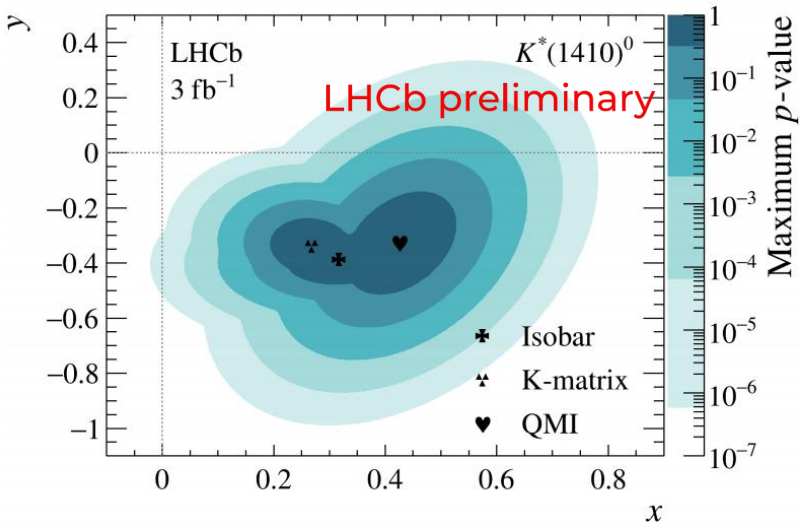

Component	HFLAV (10^{-6})	Branching fraction (10^{-6})
$B^+ \to K_2^*(1430)^0\pi^+$	$5.6^{+2.2}_{-1.4}$	$3.90 \pm 0.57 \pm 0.31 \pm 0.13$
$B^+ \to f_2(1270)K^+$	1.07 ± 0.31	$2.21 \pm 0.30 \pm 0.30 \pm 0.09$
$B^+ \to K^*(1410)^0\pi^+$	$< 45\,(90\%\,\mathrm{CL})$	$9.17 \pm 2.39 \pm 2.49 \pm 1.82$
$B^+ \to \rho_3(1690)^0K^+$	–	$1.00 \pm 0.26 \pm 0.37 \pm 0.06$
$B^+ \to K_0^*(1950)^0\pi^+$	–	$1.32 \pm 0.27 \pm 0.08 \pm 0.36$
$B^+ \to f_0(1370)K^+$†	$< 11\,(90\%\,\mathrm{CL})$	$9.67 \pm 0.70 \pm 0.23$
$B^+ \to f_0(1500)K^+$	–	$4.65 \pm 0.74 \pm 0.32$
$B^+ \to f_0(500)K^+$†	–	$1.06 \pm 0.22 \pm 0.03$
$B^+ \to f_0(1710)K^+$†	–	$0.41 \pm 0.34 \pm 0.01$
$B^+ \to (\pi\pi - \pi\pi)K^+$†	–	$3.09 \pm 1.03 \pm 0.08$

Preliminary

Outline

- Introduction
- Amplitude analysis
- Physics results and implications
  - *CP* violation
  - Strong interaction modelling implications
- Conclusion

Conclusion

- **An amplitude analysis** of $B^+ \to K^+\pi^-\pi^+$ with CP violation has been performed **LHCb-PAPER-2025-067**

- ***CP* violation** **LHCb-PAPER-2025-069**
  - Observed in $B^+ \to \rho(770)^0 K^+$ and $B^+ \to f_2(1270)^0 K^+$ decays
  - Observed in $B^+ \to (S-P)K^+$ interference
  - Evidence for *CP* violation in $B^+ \to \rho_3(1690)^0 K^+$ decay
  - Evidence for *CP* violation in low-mass $\pi\pi$ S-wave region
  - Evidence for *CP* violation in $B^+ \to (S-D)K^+$ interference

- **Implications for strong-interaction modelling** **LHCb-PAPER-2025-068**
  - $B^+ \to K_0^*(1430)^0\pi^+$ BF now agrees with QCDf, resolving a longstanding puzzle
  - No additional $f_X(1300)$ contribution required
  - Ten intermediate processes observed for the first time, with improved BF precision

- **Outlook**
  - Larger datasets now available at LHCb, but need reductions of both experimental and model unc.

Thanks for your attention

Backups→